Distinguishing different paths for rearrangements on surfaces

1994 J. Phys.: Condens. Matter 6 7269

(http://iopscience.iop.org/0953-8984/6/36/011)

J. Phys.: Condens. Matter 6 (1994) 7269–7286. Printed in the UK

Distinguishing different paths for rearrangements on surfaces

L Kjeldgaard† and J C Schön‡

Niels Bohr Institutet, NBIfAFG Copenhagen University, Blegdamsvej 17, DK-2100 København Ø, Denmark

Received 3 May 1994

Abstract. There exist a variety of theoretical models that can be employed in the description of the rearrangements on surfaces. Prominent examples are the coarsening model of Lifshitz and Slyozow and the diffusion aggregation process due to von Smoluchowski. We perform computer simulations on the merging of pores in a two-dimensional Ising model with the goal of determining the conditions under which the system follows one of these paths during reconstruction. The parameters that are varied during the investigation are the size of the pores, their separation and the temperature of the system. It is found that with increasing temperature the transition line moves towards larger distance and radii and broadens for high temperatures.

1. Introduction

Both in two-dimensional and three-dimensional systems a multitude of processes exist that to some degree show coarsening behaviour. These range from the movement and accumulation of He bubbles in the steel walls of nuclear reactors [1–3] and coagulation of, for example, protein [4] over the Ostwald ripening during sintering [5] and recrystallization processes to the reconstruction of surfaces after, for example, MBE or ion bombardment [6]. The common element in all these processes is the formation of larger domains—bubbles or pores consisting of atoms or vacancies—that can move, merge, split and/or interact via emission and reabsorption of carriers (be it atoms or vacancies). The development of the size distribution of such domains has been studied both experimentally [7–10] and theoretically [11–14] for a long time.

The growth of larger domains can occur in two basic ways: through coalescence of smaller domains or through the emission and reabsorption of individual carriers as, for example, in Ostwald ripening. All other models seem to be based on variations or combinations of these two mechanisms. Two models, each of which describes in an idealized form one of these mechanisms, were originally proposed by von Smoluchowski [12] and Lifshitz and Slyozow [15], respectively. The former assumes that no carriers are emitted once they are part of a larger pore, and that the growth of the pores takes place via the slow diffusion of the whole pores and their merger upon encountering one another. In contrast, the latter supposes that the distances between the pores are so large that the motion of the pores can be ignored, and the only interaction among them is via a 'sea' of carriers that permeate the host matrix and which are being emitted and absorbed constantly by the

† Current address: HLRZ, Forschungszentrum Jülich, D-52425 Jülich, Germany.
‡ Institut für Anorganische Chemie, Universität Bonn, Gerhard-Domagk-Straße 1, D-53121 Bonn, Germany.

0953-8984/94/367269+18$19.50

individual pores. Both models have in common that in their purest version, the time scale for shape changes of the pores is very short compared to all other processes.

Clearly, if the pores are so close that they are nearly touching one another, then a von Smoluchowski-like process will occur, while for pores that are infinitely far apart no direct contact is possible, and the interaction must happen via individual carriers. It appears reasonable to suggest that there should be some transitional distance that separates the two extremes. Such a critical distance will presumably be a function of the size of the pores and the temperature. Whether this transition is sharp or diffuse might be difficult to establish, since no system—be it real or simulated by computer—will in all likelihood fulfill all the implicit assumptions of the models and also be able to encompass both of them. In particular, the shape of the pores and their locomotion typically do not fully obey the simple pictures used to describe them.

Keeping this in mind, we have studied the movement of pores of various sizes and their interaction and eventual merger using a two-dimensional Ising model. We find a linear transition line in the radius against separation distance phase diagram, with decreasing slope for increasing temperature. We also observe a broadening of the transition line, to a transition region in the highest temperature run.

Furthermore, we have selected initial configurations containing many pores deep within each of the two regimes, and studied the time evolution of these systems. We find that the average size of the pores grows as $t^{0.37}$ in the case of the 'Smoluchowski-type' mechanism, while the growth follows a $t^{0.33}$ law for the 'Lifshitz–Slyozow-type' mechanism. We show that these results agree with simple models of the time evolution of such systems.

2. Procedure of the computer simulations

We have performed constant density simulations of two pores of identical initial size, on a square lattice. Its size was varied according to the size of the pores in order to keep the vacancy density constant.

The pore radii, r, were increased from one to six (in units of the lattice constant) and the lattice from 20×20 to 120×120. The initial distances, d, between the two pores varied from two to nine lattice constants.

Three different temperature values were chosen, $T = 0.25$, $T = 0.375$ and $T = 0.5$, in units of the nearest neighbour interaction, J_1.

After having determined the regions in (r, d) space, where each of the two different regimes apply, i.e. growth through coalescence and single carrier emission+absorption, respectively, we performed simulations using many pores. The initial conditions were always chosen to ensure that only one of the two mechanisms would apply throughout a given run. Up to fifty pores were used in order to get a reasonably smooth time evolution of the ensemble of pores.

In addition, we determined the diffusion constant as a function of the radius of the pores within the context of our model system, in order to allow comparison with simple models and experimental observations.

To perform the simulations, we employed the two-dimensional lattice gas Ising model with nearest and next nearest neighbour interactions, J_1 and J_2, where we set $J_1 = 1$ and $J_2 = 1/\sqrt{2}$ for simplicity:

$$H = -J_1 \sum_{\text{nn}} \sigma_i \sigma_j - J_2 \sum_{\text{nnn}} \sigma_i \sigma_j. \tag{1}$$

For each run the number of vacancies were kept constant. The diffusional dynamics of

the atoms/vacancies were calculated using the random exchange of nearest neighbours weighted according to the Metropolis criterion. Periodic or reflecting boundary conditions were employed depending on the problem. The main calculations were done on a VMS mainframe taking approximately 18 months, and reached up to 10^7 timesteps each.

3. Results of the simulations

3.1. Diffusion of single islands

In order to determine the diffusion coefficient as a function of its radius within the context of our model, we have plotted the mean displacement squared versus the number of timesteps. Its slope is proportional to the diffusion coefficient of the pore under consideration. Repeating this step at constant temperature for several radii, r, we found that

$$D(R) \propto R^{-4} \tag{2}$$

as shown in figure 1. The statistical error in the values of the diffusion coefficients ranges from 10^{-4} to 10^{-2}, and have been indicated by error bars in the figure.

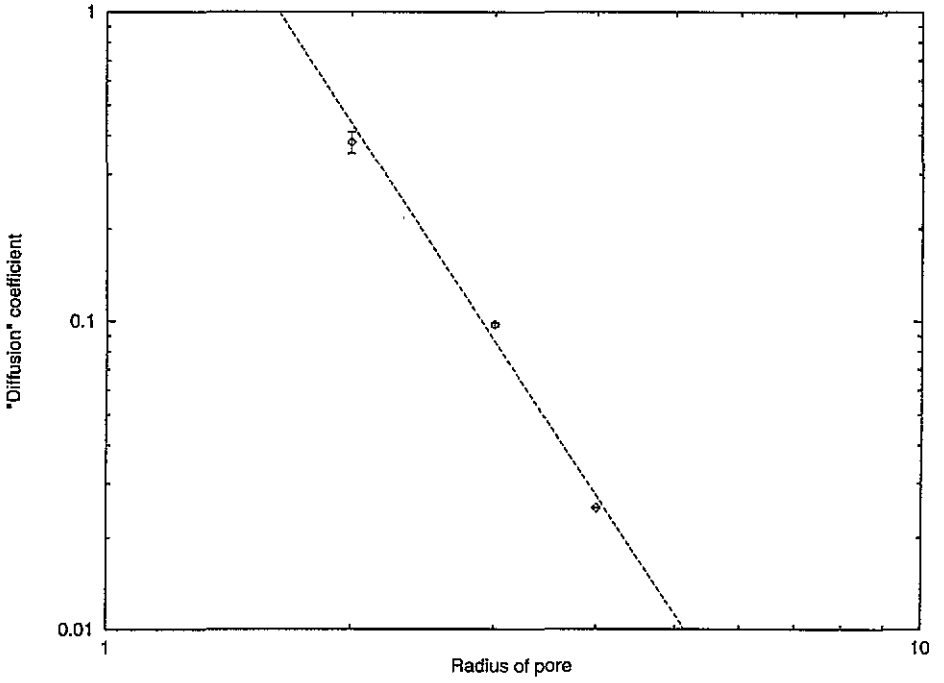

Figure 1. The diffusion constant as a function of the radius of the pore.

3.2. Transition line between merger and emission+absorption-like behaviour

Figures 3–5 depict the region in the (r, d) plane that was covered by the simulations for three different temperatures. Each run for a pair of pores of radius r and initial separation distance d was carefully monitored and classified according to the coalescence mechanism. All instances where a continuous decrease in the size of one pore occurred together with a smooth increase in the size of the other, were denoted as a 'Lifshitz–Slyozow-type' process.

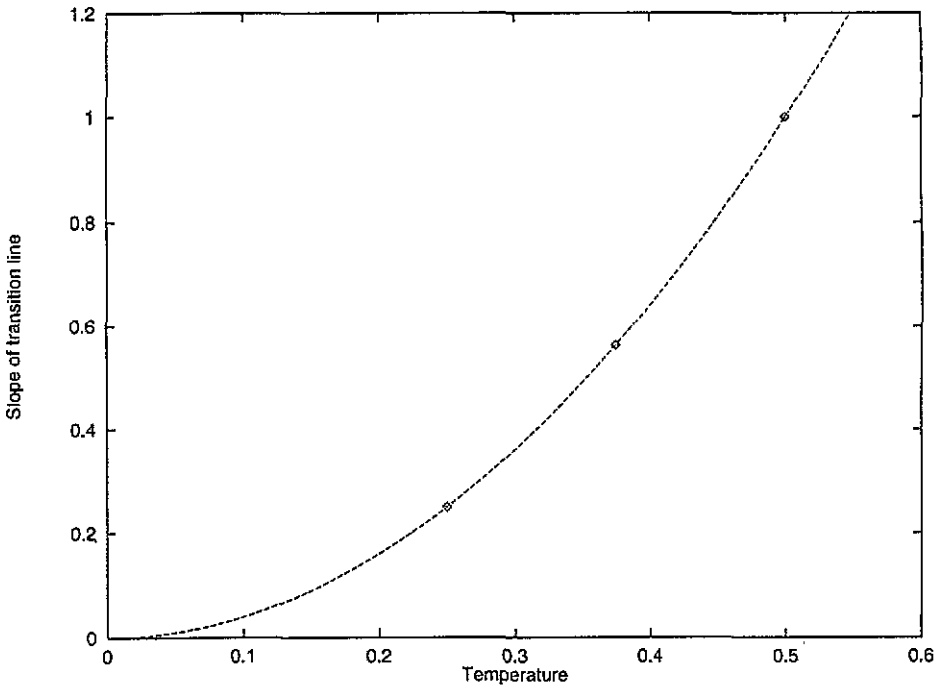

Figure 2. The temperature dependence of the slope of the transition line.

In contrast, when an abrupt merger was seen, usually accompanied by the creation of a highly elongated intermediate configuration, the coalescence was classified as a 'Smoluchowski-type' merger.

As can be seen in the figures, the section of the transition region accessible to our simulations can be described by a straight line. Clearly, for the highest temperature, $T = 0.5$, the transition line has broadened into a transition zone. Nevertheless, the centre of this region can be described approximately by $d^{tr} = \alpha r$, where $\alpha = 1$.

3.3. Multi-pore simulations

Finally, we have set up runs with many (fifty) identical pores, and followed their time evolution under conditions that corresponded either to the merger-like or the emission+absorption-like regimes. Figures 6 and 7 show plots of the average number of vacancies in a pore against time steps. Also shown is a power law fit of the mean cluster size. In the 'Smoluchowski' regime, the exponent equals 0.37, whereas the 'Lifshitz–Slyozow' regime shows a growth proportional to $t^{0.33}$. The standard deviation was found to be 0.11 for the merger-like and 0.07 for the emission+absorption-like process.

4. Comparison with simple analytical models

In order to gain further understanding of the simulations, we compare the results with the predictions of simple models for the diffusion behaviour, the analytical form of the transition line and models for the early time behaviour of merger-like and emission+absorption-like processes.

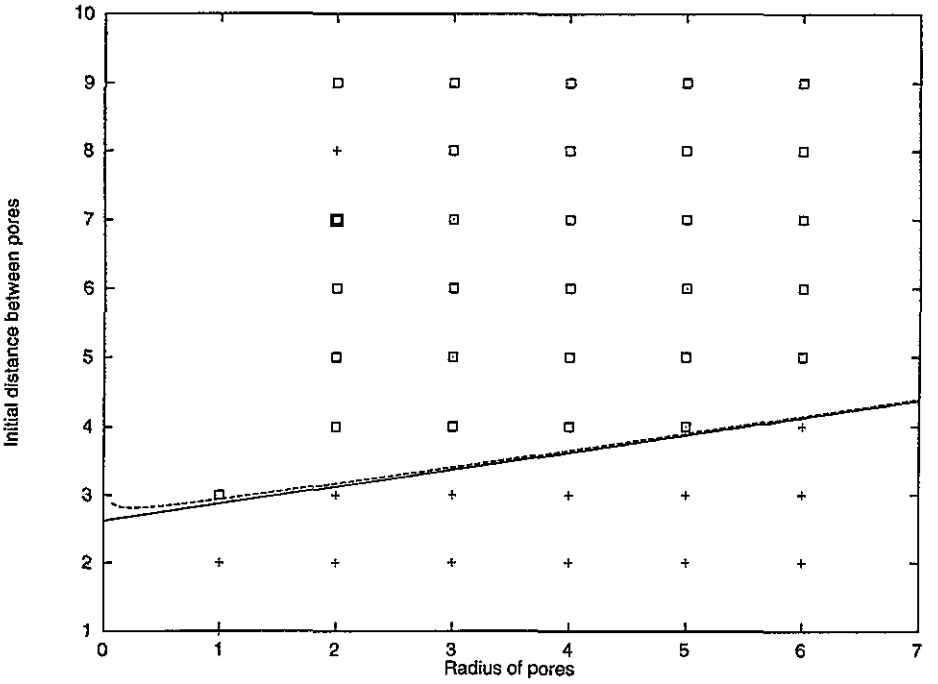

Figure 3. The transition line for $T = 0.25$, fitted with: (i) $d^{tr} = \alpha'(T)r + \gamma'(T), \alpha'(0.25) = 0.25, \gamma'(0.25) = 2.625$ (solid line) (ii) $d^{tr} = \alpha(T)r + 2\sqrt{\beta(T)/r} + \gamma(T), \alpha(0.25) = 0.25, \beta(0.25 = 0.001, \gamma(0.25) = 2.625$ (dashed line). The crosses indicate the merger-like region and the squares mark what we classified as the emission+absorption-like region.

4.1. The diffusion coefficient

In appendix A, we present the adaptation of several standard models for the size dependence of the diffusion constant to the two-dimensional case. We can distinguish the following cases

(a) perimeter transport: $D_{\text{pore}} \sim D_{\text{ind}} r^{-3}$
(b) area transport: $D_{\text{pore}} \sim D_{\text{ind}} r^{-2}$
(c) vapour transport: $D_{\text{pore}} \sim D_{\text{ind}} r^{-2}$, $D_{\text{pore}} \sim D_{\text{ind}} r^{-1}$
(d) local equilibrium transport: $D_{\text{pore}} \sim D_{\text{ind}} r^{-4}(r + b(T))$.

The size dependence of the diffusion coefficient that was observed during the simulations agree only with model (d), for small pores. We would expect that for larger pores a standard perimeter transport would be observed. Further studies of larger pores and the temperature dependence of the diffusion constant would be necessary in order to decide whether this expectation holds true.

4.2. The transition line

A simple derivation of the location of the transition line can be given as follows. For two pores of radius r to merge, they have to be within a centre-to-centre distance $d_{cc} = 2r + f(r, T)$, where $f(r, T)$ is a measure of the deformation due to the shape fluctuations a pore will exhibit at a temperature T. Thus, the pores will have to diffuse a distance $d - f(r, T)$, where d is the initial surface to surface separation of the initially

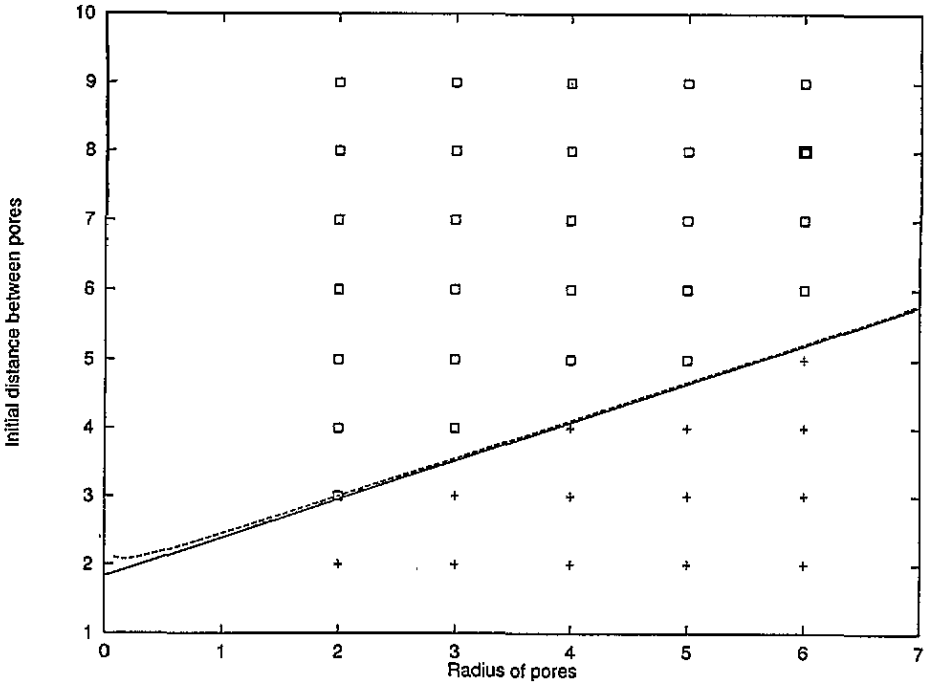

Figure 4. The transition line for $T = 0.375$, fitted with: (i) $d^{tr} = \alpha'(T)r + \gamma'(T), \alpha'(0.375) = 0.5625, \gamma'(0.375) = 1.83$ (solid line) (ii) $d^{tr} = \alpha(T)r + 2\sqrt{\beta(T)/r} + \gamma(T), \alpha(0.375) = 0.5625, \beta(0.375 = 0.001, \gamma(0.375) = 1.83$ (dashed line). The crosses indicate the merger-like region and the squares mark what we classified as the emission+absorption-like region.

circular pore. With a diffusion constant $D(r)$, the time necessary for merging t_{merge} equals

$$t_{merge} = \frac{(d - f(r,T))^2}{4D(r)}. \tag{3}$$

Of course, if $d < f(r,T)$, the merger will be instantaneous, i.e. $t_{merge} = 0$.

For the appropriate time scale in the emission+absorption-like process, we may concentrate on the survival time of a pore of radius r during a 'Lifshitz–Slyozow-type' coarsening process. Since the average radius $\bar{a}(t)$ is proportional to the critical radius $a_{cr}(t)$ to survive up to a time t and $\bar{a}(t)$ is proportional to $t^{1/3}$, we can relate the time for a pore to vanish t_{van} to the radius of the pore [14]

$$t_{van} = \frac{9}{4b(T)c_{0\infty}D_{ind}}\bar{a}^3. \tag{4}$$

Here $b(T)$ is defined in Appendix C, equation (C1). Equating t_{merge} and t_{van}, we find the equation for the transition line:

$$d^{tr}(r) = f(r,T) + \sqrt{\frac{9D(r,T)r^3}{b(T)c_{0\infty}D_{ind}}}. \tag{5}$$

For the example in this study, $D(r) \sim D_{ind}r^{-4}$. If, in addition, the diffusion proceeds according to mechanism (d) of section 4.1, we note that the term under the square root sign in equation (5) should be only weakly dependent on the temperature.

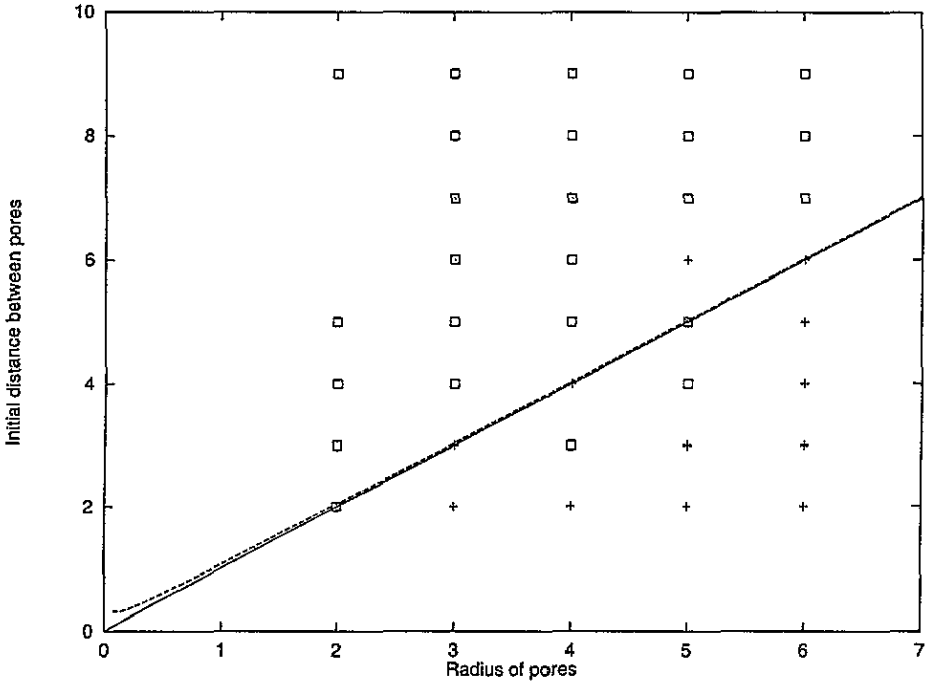

Figure 5. The transition line for $T = 0.5$, fitted with: (i) $d^{tr} = \alpha'(T)r + \gamma'(T), \alpha'(0.5) = 1.0, \gamma'(0.5) = 0.0$ (solid line) (ii) $d^{tr} = \alpha(T)r + r\sqrt{\beta(T)/r} + \gamma(T), \alpha(0.5) = 1.0, \beta(0.5 = 0.001, \gamma(0.5) = 0.0$ (dashed line). The crosses indicate the merger-like region and the squares mark what we classified as the emission+absorption-like region.

Furthermore observations of the shape fluctuations suggest that $f(r, T) = \alpha(T)r + \gamma(T)$ with $d\alpha/dT > 0$. Thus we expect the transition line to have the functional form

$$d^{tr}(r) = \alpha(T)r + 2\sqrt{\frac{\beta(t)}{r}} + \gamma(T) \tag{6}$$

where $\beta(T)$ should at most be proportional to T. For $r \to 0$ or ∞, $d^{tr} \to \infty$. There exists one minimum which is located at

$$\begin{aligned} R_{min} &= \sqrt[3]{(\beta/\alpha^2)} \\ d^{tr}_{min} &= 3\sqrt[3]{\alpha\beta} + \gamma(T). \end{aligned} \tag{7}$$

This derivation agrees with the results shown in figures 3–5, if one assumes that $R_{min} < 2$, such that our simulations are already in the appropriate straight line segment of the transition line.

Fitting the data to this functional form we found for $\alpha(T)$, $\beta(T)$ and $\gamma(T)$

$$\begin{aligned} \alpha(T) &= 4T^2 \quad \text{(cf. figure 2)} \\ \beta(T) &= \frac{1}{1000} \\ \gamma(T) &= 5\sqrt{\left|\frac{1}{2} - T\right|}. \end{aligned} \tag{8}$$

The location of the transition line according to equations (6)–(8) has been indicated by the dashed lines in figures 3–5.

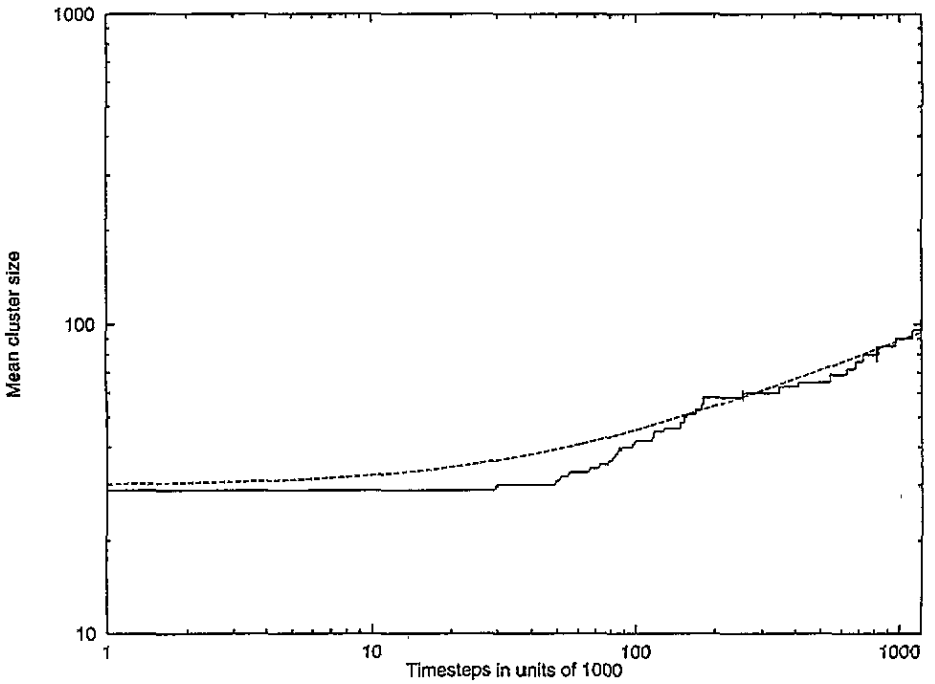

Figure 6. Time evolution of the mean cluster size in the emission+absorption-like regime (solid line). The dashed line indicates the fit to a $\bar{M}(t) = \bar{M}(0)(1 + kt)^{1/3}$ with $\bar{M}(0) = 30.0$, and $k = 0.025$.

4.3. Merger-like growth

In Appendix B, we derive a differential equation for the number of pores present at time t for an ensemble that coalesces via the diffusion and merger of whole pores. The derivation is appropriate for early to intermediate times and adapts the original arguments of von Smoluchowski to the case under consideration. We find that the average size of the pores grows as $t^{1/3}$, which compares reasonably well with the observed growth law of $t^{0.37}$.

4.4. Emission+absorption-like growth

In Appendix C, we derive again a differential equation for the number of pores present at time t for an ensemble that coalesces through emission and absorption of vacancies. The derivation is based on a separation of time scales, and the assumption that during the early stages of the coarsening process the pores are distributed rather densely resulting in a shielding of pores by their immediate neighbours. The resulting growth law for the average size of the pores is found to be $M(t) = (kt + M_0^3)^{(1/3)}$, which very closely reproduces the functional form of the observed growth.

5. Discussion and outlook

It was seen in the preceding section that the results of the simulations agree well with the predictions of the simple models. This agreement continues for simulations with different overall vacancy densities, but so far no systematic study of the density dependence of the

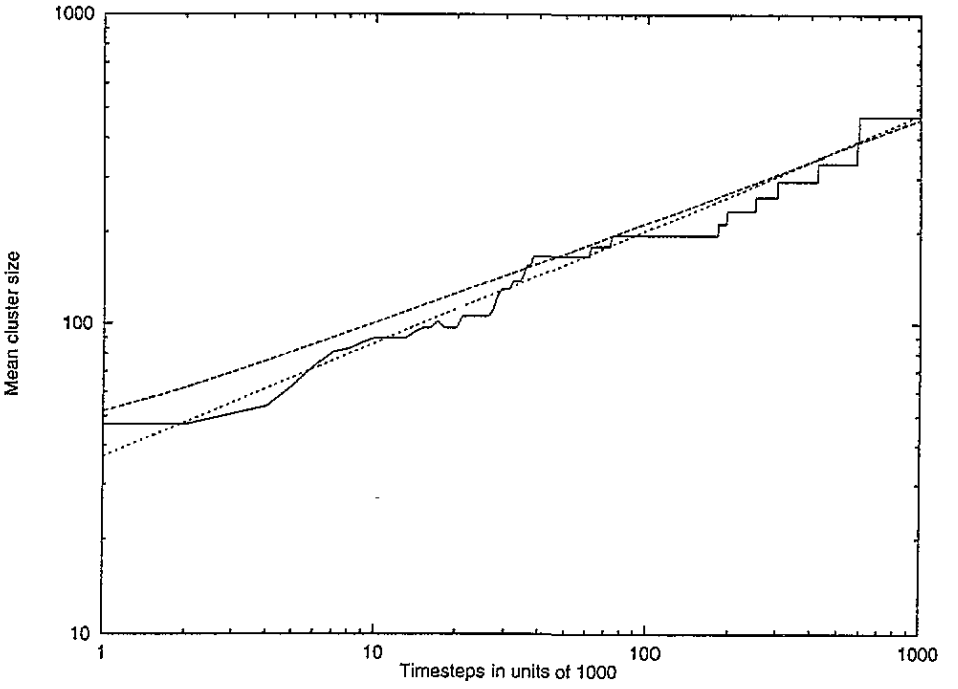

Figure 7. Time evolution of the mean cluster size in the merger-like regime (solid line). The dashed line indicates the fit to a $\bar{M}(t) = \bar{M}(0)(1+kt)^{1/3}$ with $\bar{M}(0) = 35.0$, and $k = 2.3$, while the dotted line shows the best fit to the $\bar{M}(t) \propto t^{0.37}$, with proportionality factor $\bar{M}(0) = 37.0$.

prefactors in the growth models and the parameters in the formula of the transition line has been performed.

An interesting observation during the ensemble runs is the fact that since $N(t)$ decreases with time, and thus the average distance between the pores increases, a transition from a merger-like to an emission+absorption-like behaviour occurs at some point in time. It was therefore necessary to choose the initial conditions for the 'Smoluchowski-type' ensemble simulations very carefully in order to be able to study a pure merger-like process. We note that this is a consequence of the size dependency of the diffusion coefficient we observed during the simulations.

The question whether the simple models we proposed in section 4 are applicable beyond the simulations presented in this paper, depend on two issues

(i) The degree to which the prefactors and parameters may be connected to other numerical and/or experimental quantities

(ii) The degree to which the models can be generalized to different dimensions and/or different functional forms of 'empirical' laws entering the model (e.g. the size dependence of the diffusion coefficient).

Whether the interpretation that the size dependence of the diffusion coefficient follows from e.g. mechanism (d) of section 4.1 is correct, could be determined by studying the limiting behaviour of $D(r)$ for large r, which should be approximately $D(r) \sim r^{-3}$. As with other suggestions made below, this issue awaits further investigations. However, the observed weak temperature dependence of $\beta(T)$ in the equation of the transition line (equation (6)) indicates that our model for $D(r)$ is at least approximately correct. In this

context we note that the data obtained by Poulsen *et al* [10] show a cross over to $D(r) \sim r^{-5}$, in their study of diffusion of sodium inclusions in a three-dimensional platinum matrix.

Clearly all the pore diffusion mechanisms in Appendix A and the model for the transition line can be easily generalized to m dimensions (most of the diffusion mechanisms had been derived for the case of three dimensions originally). In order to validate these models, it would be desirable to repeat our simulations in e.g. three dimensions and, if possible, for larger regions of the (r, d) space. In addition, we feel that interesting phenomena might occur for temperatures and densities near the equilibrium phase transition of the Ising model. Already some indications may be seen in the existence of the transition zone for $T = 0.5$, where $\gamma(T)$ reaches zero in a singular manner.

In this context it should be mentioned that the shape of the transition line can change as the distribution of pores evolves. Equation (6) was derived using equation (4), which strictly holds [14]—up to correction terms—only in the Lifshitz–Slyozow model for isolated pores. If one includes the shielding effects during the early stages of the 'Lifshitz–Slyozow-type' process, one finds, according to Appendix C and our simulations,

$$d^{\alpha} = \alpha'(T)r + \gamma'(T) \tag{9}$$

instead of equation (6). Thus, as the coarsening proceeds and shielding effects become less prominent, the transition line will change from equation (9) to equation (6). Note that since $\beta(T)$ in equation (8) was found to be very small, the transition line observed in our simulations can be fitted both to equation (6) and equation (9), with $\alpha'(T) \approx \alpha(T)$ and $\gamma'(T) \approx \gamma(T)$.

Concerning the two growth models in Appendices B and C, we note that the 'Lifshitz–Slyozow-type' model obviously shows no dependence on the functional form of $D(r)$. If we repeat the calculations in Appendix C with the same degree of approximations for different dimensions m we find a growth law of $\bar{M} \propto t^{m/(4+m)}$. For the case of two dimensions, we also consider the case of $t \to \infty$, i.e. no shielding is present and all the pores interact equally with each other. Note that this would be different from the classical Lifshitz–Slyozow model, where the interaction explicitly occurs through the free vacancies in the matrix. If now the same estimates for the behaviour of M_0 and $\bar{a}$ hold, then $\bar{M} \propto t^{1/2}$. However, for large t, M_0 will probably grow more slowly than $\bar{M}$. Assuming that $M_0 \propto \bar{a} \propto \sqrt{\bar{M}}$, we find $\bar{M} \propto t^{2/3}$. The latter result would agree with the result of the standard two-dimensional Lifshitz–Slyozow model, while the former lies halfway between the shielding model and the Lifshitz–Slyozow result.

The extensions of the 'Smoluchowski-type' model are more involved, since both the functional form of $D(r)$ and the dimension m play an important role in the derivation. Assuming again a sharply peaked initial pore size distribution and $D(r) \sim r^{-\epsilon}$, we find for intermediate times t that

$$\frac{\mathrm{d}N}{\mathrm{d}t} \propto -N^2 i_{\max}^{(-\epsilon/m)} i_{\max}^{(m-2)/m}$$

and thus $\bar{M}$ approximately follows the growth law $\bar{M} \propto t^{m/(2+\epsilon)}$.

We note here that while the calculation in Appendix C is rather straightforward and the approximations are well controlled by the separation of time scales argument, the approximations involved in Appendix B are more subtle. They involve both the short time limit in order to deal with the gradual change of the pore size distribution and also the (somewhat) long time limit (used already by von Smoluchowski in his original derivation) in order to avoid having to deal with the shielding effects directly. If one were to try and take this into account—as in Appendix C—and if one keeps only the first term in the short time expansion in the diffusional flow (equations (B6), (B10)), one finds $\bar{M} \propto t^{m/(2\epsilon-2)}$. We

observe that for the case investigated in the simulations, $\epsilon = 4$, the behaviour of $\bar{M}$ in the two models is identical. Furthermore, let us assume that mechanism (d) (cf. section 4.1) for the size dependence of $D(r)$ holds, and thus for intermediate radii of the pores, $3 < \epsilon < 4$. Then we would expect that the growth exponent of $\bar{M}$ should be slightly larger than 1/3 and slowly increase with time as the surviving pores grow. The exponent observed during the simulations would be consistent with this interpretation.

The original motivation of this work has been the attempt to understand which paths a physical system would follow during surface and grain boundary evolution, and thus which model for the growth kinetics of the pores and/or grains would be most appropriate. Once this is known, one might be able to estimate the effects due to changes in the controlling parameters such as the temperature. This should allow more control in, for example, the rearrangements on surfaces after the deposition of atomic layers from the gas phase or the bombardment with ions.

Beyond these relatively applied issues, we feel that the models we present could be used to address more mathematical questions, like the solution of the von Smoluchowski equations in three dimensions for kernels (i.e. diffusion coefficients D_{ij}) that depend on the radius by some inverse power, ϵ, $r^{-\epsilon}$. This might complement work by Hendriks et al [16], which appears to apply only to the case $D(r) \sim r^{+\epsilon}$. Finally, the methods we present to deal in a local average fashion with shielding effects should also be useful in standard diffusion-reaction and ensemble growth models.

Acknowledgments

The authors would first and foremost like to thank the system manager: Dr Björn S Nilsson—and all the other users—at NBIVAX, Copenhagen, for their great patience and endurance. For discussions, we would like to thank Dr Paolo Sibani, Odense University, Denmark and Dr M Schreckenberg, University of Cologne, Germany.

Appendix A. Movement of the pores

In the literature [11] a number of transport mechanisms for the movement of bubbles of e.g. He in steel have been suggested: surface transport, volume transport and vapour transport (both at constant pressure and constant surface tension). All these mechanisms are based on the assumption that the diffusion of a large pore occurs via the collective effect of the diffusion of single atoms belonging to the matrix or the bubble. Their derivation can be adapted to the two-dimensional case. We note that the displacement of one atom or vacancy by a distance λ corresponds to the movement of the whole pore by a distance $\lambda_p = \lambda/N$, where N equals the number of vacancies in the pore. On the other hand, since there are M atoms 'available' to attempt a move within a time step, where M is a function of the transport mechanism, the jump frequency of the pore Γ_p is given by

$$\Gamma_p = M\Gamma_{ind}. \tag{A1}$$

Finally one knows the diffusion coefficient of the diffusing species for each of these mechanisms, i.e. we know the relation connecting the jump frequency of an individual carrier Γ_{ind}, the stepsize λ during the diffusion process and the single carrier diffusion coefficient D_{ind},

$$D_{ind} = \tfrac{1}{4}\Gamma_{ind}\lambda^2. \tag{A2}$$

Together with the definition of the (two-dimensional) pore diffusion coefficient as

$$D_p = \tfrac{1}{4}\Gamma_p \lambda_p^2 \tag{A3}$$

we can derive an expression for D_p for the various transport mechanisms. We note that for simplicity it is typically assumed that λ corresponds approximately to the mean diameter of a single representative of the diffusing species, and that the pore is approximately disk shaped with radius r. It follows that

$$N = \frac{\pi r^2}{\lambda^2}. \tag{A4}$$

A.1. Perimeter transport

Here, it is assumed that the transport occurs via the movement of atoms of the host matrix belonging to a thin zone of thickness λ along the perimeter of the pore. Thus

$$M = \frac{2\pi\lambda r}{\lambda^2} = \frac{2\pi r}{\lambda} \tag{A5}$$

and it follows from equations (A1)–(A3) that

$$D_p = \frac{2D_{ind}\lambda^3}{\pi r^3}. \tag{A6}$$

A.2. Area transport

We assume that the vacancies are diffusing through the whole area of the host matrix. Typically it is assumed that all the vacancies can participate; so we have

$$M = N \tag{A7}$$

and thus

$$D_p = \frac{D_{ind}\lambda^2}{\pi r^2}. \tag{A8}$$

A.3. Vapour transport

It is assumed that atoms of the host matrix evaporate from the perimeter of the pore and diffuse through the (vapour filled) pore to the other side. Thus

$$\lambda = \lambda_g \tag{A9}$$

$$N = \frac{\pi r^2}{\lambda_g^2}. \tag{A10}$$

In order to determine M, we note that the evaporated host atoms can be treated as an ideal gas and that their number is determined by their vapour pressure, P_v:

$$P_v = \frac{P_g M}{N} = \frac{M k_B T}{\pi r^2}. \tag{A11}$$

Then, we find that

$$D_p = \frac{D_{ind} P_v \lambda_g^4}{\pi k_B T r^2} \tag{A12}$$

where an explicit temperature dependence has entered. In this situation it was implicitly assumed that the gas pressure, P_g, within the pore is independent of the size of the pore. Alternatively, the gas pressure may balance the surface tension σ of the pore, resulting in

$$P_g = \frac{\sigma}{r}. \tag{A13}$$

It follows that

$$M = \frac{NrP_v}{\sigma} \tag{A14}$$

and thus

$$D_p = \frac{D_{ind}P_v\lambda_g^2}{\pi\sigma r}. \tag{A15}$$

A.4. Local equilibrium transport

The last transport mechanism is based on the assumption that local equilibrium exist between the pore of radius r and the cloud of vacancies surrounding it. If these vacancies dominate the pore diffusion, the number of participating vacancies is approximately given by

$$M = c_{0r}2\pi\lambda r = c_{0\infty}2\pi\lambda(b(T) + r). \tag{A16}$$

The second equality follows from equation (C1). It follows that the pore diffusion coefficient equals:

$$D_p = \frac{2D_{ind}c_{0\infty}\lambda^5(b(T) + r)}{\pi r^4}. \tag{A17}$$

We note that for large radii this mechanism becomes essentially indistinguishable from the perimeter transport.

Appendix B. Early time growth law for merger-like processes

We derive an approximate formula for the number of pores at time t, $N(t)$, which is valid for small to intermediate times in the von Smoluchowski picture.

We begin by considering the flow across the perimeter of a disk with radius R. The two-dimensional diffusion equation for the pore density u with the boundary conditions:

$$\begin{aligned} u &= c \quad \text{for} \quad t = 0, \quad r > R \\ u &= 0 \quad \text{for} \quad t > 0, \quad r = R \end{aligned} \tag{B1}$$

can be solved by separation of variables via the ansatz

$$u = \int_0^\infty h(\alpha; r, t)d\alpha, \qquad h(\alpha; r, t) = e^{-\alpha t}g(\alpha, r) \tag{B2}$$

where $g(\alpha, r)$ is the solution to the differential equation

$$D\left(\frac{d^2g}{dr^2} + \frac{1}{r}\frac{dg}{dr}\right) = -\alpha g. \tag{B3}$$

The result is [17]:

$$u(r) = \frac{2}{\pi}\int_0^\infty \exp(-Dk^2t)\frac{Y_0(kr)J_0(kR) - Y_0(kR)J_0(kr)}{k(Y_0^2(kR) + J_0^2(kR))}dk \tag{B4}$$

where $\alpha = k^2$.

The amount of diffusional substance F crossing the perimeter at $r = R$ in unit time is given by

$$F(t) = 2\pi RD\frac{\partial u}{\partial r} = \frac{8cD}{\pi}\int_0^\infty \exp(-Dk^2t)\frac{1}{k(Y_0^2(kR) + J_0^2(kR))}\mathrm{d}k. \tag{B5}$$

Since we are interested in relatively short times, we expand $F(t)$ for small t:

$$F(t) \approx 2\pi cD\left(\frac{R}{\sqrt{\pi Dt}} + \tfrac{1}{2} + \mathcal{O}(\sqrt{t})\right). \tag{B6}$$

The total amount of material $M(\Delta t)$ added in the time Δt then equals

$$M(\Delta t) = 2\pi Dc\left(\frac{2R\sqrt{\Delta t}}{\sqrt{\pi D}} + \tfrac{1}{2}\Delta t\right). \tag{B7}$$

Following the arguments of von Smoluchowski [12], the probability $P(t)$ that for a given particle no merger has occurred within a time t, is given by

$$P(t) \approx \exp\left[-\pi cD\left(\frac{4R\sqrt{t}}{\sqrt{\pi D}} + t\right)\right]. \tag{B8}$$

Assuming that the particles (i.e. the pores) can be treated as independent, the number density $\nu(t)$ of those which have not merged equals

$$\nu(t) = c\exp\left[-\pi cD\left(\frac{4R\sqrt{t}}{\sqrt{\pi D}} + t\right)\right]. \tag{B9}$$

Their decrease is given by

$$\frac{\mathrm{d}\nu}{\mathrm{d}t} = -\nu\pi cD\left(\frac{2R}{\sqrt{\pi Dt}} + 1\right). \tag{B10}$$

For the intermediate time scale that we are interested in we make the assumptions that we can take the slow decrease in the number of available particles into account by replacing c by ν, and that we should be able to drop the $2R/\sqrt{\pi Dt}$ term:

$$\frac{\mathrm{d}\nu}{\mathrm{d}t} = -\pi D\nu^2. \tag{B11}$$

Since both merging particles, i and j, are in motion, the diffusion constant in the preceding equation should be replaced by the sum of the individual diffusion constants, $D_{ij} = D_i + D_j$. Finally we take into account that all pores can move and merge, i.e. the primary pores can merge not only with themselves, but with pores of all sizes. This can be described by a set of chemical reaction equations

$$\frac{1}{\pi}\frac{\mathrm{d}\nu_k}{\mathrm{d}t} = \tfrac{1}{2}\sum_{i+j=k}^{N_{\mathrm{tot}}} D_{ij}\nu_i\nu_j - \sum_{j=1}^{N_{\mathrm{tot}}} D_{jk}\nu_k\nu_j \tag{B12}$$

also known as the von Smoluchowski equation for a finite system.

N_{tot} is the size of the largest pore possible containing all the vacancies present in the system. As long as $N_{\mathrm{tot}} \to \infty$, or at least the times considered are short enough such that $\nu_i(t) = 0$ for $i > L$ with $L \ll N_{\mathrm{tot}}$, equation (B12) is approximately correct.

The total number of pores per unit volume at time t is given by

$$M_0(t) = \sum_j^{N_{\mathrm{tot}}} \nu_j(t). \tag{B13}$$

This leads to a differential equation for $M_0(t)$

$$\frac{dM_0(t)}{dt} = 2\pi \left(\tfrac{1}{2} \sum_{i=1}^{N_{tot}} \sum_{j=1}^{i-1} (D_i + D_{i-j}) \nu_i \nu_{i-j} - \sum_{i=1}^{N_{tot}} \sum_{j=1}^{N_{tot}} (D_i + D_j) \nu_i \nu_j \right) \tag{B14}$$

which can be rewritten as

$$\frac{dM_0(t)}{dt} \approx 2\pi \left(\sum_{i=1}^{N_{tot}} \sum_{j=1}^{i-1} D_i \nu_i \nu_{i-j} - 2M_0(t) \sum_{i=1}^{N_{tot}} D_i \nu_i \right). \tag{B15}$$

An exact solution of this equation does not appear to be feasible. However, we may make some reasonable assumptions based on the qualitative picture that; (a) $\nu_i(t) = 0$ for $i > L$ with $2L < N_{tot}$; (b) $\nu_i(t)$ as a function of i is rather strongly peaked in the neighbourhood of a value $i_{max}(t)$; (c) for our simulations, $D(r) \propto r^{-4} \propto i^{-2}$.

From (b) we can conclude that $M_0(t) \approx \nu_{i_{max}}(t)$ and $i_{max}(t) \approx N_{tot}/M_0(t)$. From (a) and (c) it follows that by expanding and rearranging the double sum in equation (B14) we can approximate the first sum in equation (B15) as:

$$\sum_{i=1}^{N_{tot}} \sum_{j=1}^{i-1} D_i \nu_i \nu_{i-j} \approx M_0(t) \sum_{i=1}^{N_{tot}} D_i \nu_i. \tag{B16}$$

Next we find

$$\sum_{i=1}^{N_{tot}} D_i \nu_i \propto \sum_{i=1}^{N_{tot}} \frac{\nu_i}{i^2} \tag{B17}$$

$$\approx \frac{\nu_{i_{max}}}{i_{max}^2} \tag{B18}$$

$$\approx \frac{M_0(t)^3}{N_{tot}^2}. \tag{B19}$$

Collecting all the proportionality factors into one constant, A, we then get the following differential equation for $M_0(t)$ for early times:

$$\frac{dM_0(t)}{dt} = -\frac{3A}{N_{tot}^3} M_0(t)^4. \tag{B20}$$

Solving this equation, we find

$$M_0(t) = \left(\frac{A}{N_{tot}^3} t + N(0)^{-3} \right)^{(-1/3)}. \tag{B21}$$

Since mass conservation holds, the first moment, N_{tot}, is constant, and we have that the mean cluster size, $\bar{M}(t)$—which is the fraction of the zeroth and the first moment, grows inversely proportional to $M_0(t)$:

$$\bar{M}(t) = \frac{N_{tot}}{M_0(t)} = (At + \bar{M}(0)^3)^{(1/3)}. \tag{B22}$$

Appendix C. Early time growth in emission+absorption-like processes

During the early time development of a system of pores that interact via the emission and absorption of individual vacancies, several effects occur that are not present in the standard Lifshitz–Slyozow model: there is no steady state equilibrium between the vacancy density close to the pores and the vacancy density in the regions between the pores, i.e. the pores

interact on an individual basis and not via a sea of 'free' vacancies. Furthermore, the density of pores is so high that a given pore is essentially shielded by its neighbours within a distance $d(t)$ from the rest of the system.

In order to model the development of the size distribution, and especially $M_0(t)$, the number of pores per volume, we will employ some separation of time scale arguments:

C.1. Small time scale

The fastest time scale should be the local equilibration of a pore of size M, i.e. with radius $a \sim \sqrt{M}$, with its surrounding cloud of vacancies. Thus the pore should be approximately disc shaped, and the density of vacancies may be given by the standard formula [15]

$$c_{0a} = c_{0\infty}\left(1 + \frac{b(T)}{a}\right) \qquad b(T) = \frac{2\sigma v'}{T}. \tag{C1}$$

Here, σ is the surface tension coefficient and v' the area of a single vacancy. We recall that the overall density of vacancies is chosen such that the weak oversaturation limit applies.

C.2. Intermediate time scale

The next time scale applies to the average pairwise interaction among the pores within an effective distance $d(t)$. From the calculations in Appendix B, we know that for very short times the total flow of vacancies outward from a pore of radius a equals

$$F(a,T) = \frac{c_{0a}D_{\mathrm{ind}}}{a}\left(\frac{a}{\sqrt{\pi Dt}} + \tfrac{1}{2} + \cdots\right)2\pi a \approx \frac{c_{0a}D_{\mathrm{ind}}2\pi a}{\sqrt{\pi Dt}}. \tag{C2}$$

A pore of radius a_j at distance d_{ij} from a given pore of radius a_i will be able to intercept a fraction $\alpha(T)a_j/d_{ij}$ of the flow from the emitting pore, where $\alpha(T)a_j$ is the effective cross section (it should be related to $\alpha(T)$ in section 4.2). Thus, the net flow of material from a pore i to a pore j is given by:

$$\frac{\mathrm{d}M_{i\to j}}{\mathrm{d}t} = -\frac{c_{0a_i}D_{\mathrm{ind}}2\pi a_i\alpha a_j}{d_{ij}\sqrt{\pi Dt}} + \frac{c_{0a_j}D_{\mathrm{ind}}2\pi a_i\alpha a_j}{d_{ij}\sqrt{\pi Dt}}. \tag{C3}$$

Assuming for simplicity that all pores j that interact with a given pore i may be placed at an average distance $d(t)$, we find that the change of the size M_i of pore i is described as:

$$\frac{\mathrm{d}M_i}{\mathrm{d}t} = \sum_{j=1}^{N}\frac{\mathrm{d}M_{i\to j}}{\mathrm{d}t} =$$

$$\sum_{j=1}^{N}\left(\frac{c_{0a_j}D_{\mathrm{ind}}2\pi a_i\alpha a_j}{d_{ij}\sqrt{\pi Dt}} - \frac{c_{0a_i}D_{\mathrm{ind}}2\pi a_i\alpha a_j}{d_{ij}\sqrt{\pi Dt}}\right) = \frac{g}{d\sqrt{t}}\left(bNa_i - bN\bar{a}\right). \tag{C4}$$

Here

$$\bar{a} = \frac{1}{N}\sum_{j=1}^{N}a_j \qquad g = 2\alpha c_{0\infty}\sqrt{\pi D_{\mathrm{ind}}}. \tag{C5}$$

We note that since the total number of vacancies per volume, N_t, is constant, the number of pores $N(t)$ and their average size $\bar{M}(t)$ are connected via

$$N_t = N(t)\bar{M}(t). \tag{C6}$$

Furthermore, a change in these quantities will only occur, if a whole pore has evaporated and its vacancies have been absorbed by the rest of the system. Thus, we can assume that $N(t)$, $\bar{a}(t)$ and $d(t)$ will change only slowly on the time scale $\tau(M_0(t))$ necessary for the smallest pores, of size $M_0(t)$, to vanish.

We determine $\tau(M_0(t))$ by integrating (C4)

$$\int_{M_0}^{0} \frac{\mathrm{d}M}{\sqrt{M}-\bar{a}} = \frac{bg}{d} N \int_0^{\tau} \frac{\mathrm{d}t}{\sqrt{t}}$$

$$\Leftrightarrow \sqrt{\tau} = \frac{\mathrm{d}}{bgN}\left[0 - \sqrt{M_0} - \bar{a}\ln\left(\frac{\bar{a}-\sqrt{M_0}}{\bar{a}}\right)\right] \approx \frac{\mathrm{d}}{bgN}\frac{M_0}{2\bar{a}} \tag{C7}$$

since $\bar{a} > \sqrt{M_0}$. This inequality holds, because M_0 is supposed to be the size of the smallest pores. Therefore, we find

$$\tau = \left(\frac{\mathrm{d}}{bgN}\frac{M_0}{2\bar{a}}\right)^2. \tag{C8}$$

C.3. Large time scale

On the largest time scale, we can model the change of $\bar{M}$, or N, respectively. The time dependence of $d(t)$ may be estimated by defining the effective shielding distance $d(t)$ as the radius of an area that contains enough pores, $\pi d^2 N$, with average radius $\bar{a}$ such that their total cross section, $\pi d^2 N \alpha(T)\bar{a}$, equals the circumference of this area, $2\pi d$. All pores outside this area are effectively shielded from the pore in the centre.

Therefore, $d(t)$ is related to $N(t)$ and $\bar{a}(t)$ by

$$d = \frac{2}{\alpha N \bar{a}}. \tag{C9}$$

It is more difficult to establish the behaviour of $\bar{a}(t)$ and $M_0(t)$. It can be estimated that $\bar{a}(t)$ will on the average grow as $\bar{M}^{\epsilon}$, where $1/2 < \epsilon < 1$, since $\sqrt{\bar{M}} > \bar{a} > \bar{M}/\sqrt{N_t}$. Since we begin our simulations with an equal size distribution, we may assume that this will remain rather strongly peaked around $\bar{M}$, at least for the early time behaviour we are modeling. This suggests that ϵ may be taken to be 1/2. Similarly, we can assume that $M_0(t)$ will be proportional to $\bar{M}(t)$, i.e. $M_0(t) = \delta \bar{M}(t)$.

Based on these considerations, we can derive a differential equation for $N(t)$:

$$\frac{\mathrm{d}N}{\mathrm{d}t} = -\frac{N^2}{N_t}\frac{\mathrm{d}\bar{M}}{\mathrm{d}t} \approx -\frac{N^2}{N_t}\frac{\Delta\bar{M}}{\tau} = -\frac{N^2}{N_t}\frac{M_0}{N\tau} \approx -\left(\frac{\alpha bg}{N_t}\right)^2 \frac{N^4}{\delta} = -\frac{3k}{N_t^3}N^4. \tag{C10}$$

Solving this equation yields:

$$\int_{N(0)}^{N(t)} \frac{\mathrm{d}N}{N^4} = \int_0^t \frac{3k}{N_t^3}\mathrm{d}t' \Leftrightarrow N(t) = \left(\frac{kt}{N_t^3} + \frac{1}{N(0)^3}\right)^{-1/3}. \tag{C11}$$

From this follows, using equation (C6), that the average size of the pores grows as

$$\bar{M}(t) = \frac{N_t}{N(t)} = \left(kt + \bar{M}(0)^3\right)^{(1/3)}. \tag{C12}$$

References

[1] Armstrong T R and Goodhew P J 1983 *Radiat. Eff.* 77 35–48
[2] Goodhew P J 1983 *Radiat. Eff.* 78 381–3
[3] Goodhew P J and Tylor S K 1981 *Proc. R. Soc.* 377 151–84

[4] Feder J and Jössang T 1985 *Scaling Phenomena in Disordered Systems* ed Roger Pynn and Arne Skjelstrup (New York: Plenum) 99–131
[5] German R N 1985 *Liquid Phase Sintering* (New York: Plenum)
[6] Picroux S T, Chason E and Mayer T M 1992 *MRS-Bull.* 52–7
[7] Yu Liangdeng 1992 *PhD Thesis* Ørsted Laboratory, Copenhagen University
[8] Bourdelle K K *et al* Preprint
[9] Manzke *et al* 1983 *Radiat. Eff.* **78** 327–36
[10] Poulsen J R *et al* 1994 *J. Phys.: Condens. Matter* submitted
[11] Nichols F A *J. Nucl. Mater.* 1969 **30** 143–65
[12] von Smoluchowski M 1916 *Physikalische Zeitschrift* **17** 557–71; 585–99
[13] von Smoluchowski 1918 *Zeitschrift für physikalische Chemie* **98** 129–68
[14] Schön J C and Salamon P 1994 *Phys. Rev.* B submitted
[15] Lifshitz I M and Slyozow V V 1961 *J. Phys. Chem. Solids* **19** 33–50
[16] Hendriks E M and Ernst M H and Ziff R M 1983 *J. Stat. Phys.* **31** 519–63
[17] Carslaw H and Jaeger J C 1959 *Conduction of Heat in Solids* (Oxford: Oxford University Press)